Testing the Weak Equivalence Principle with an antimatter beam at CERN

You may also be interested in:

Testing the Weak Equivalence Principle with an antimatter beam at CERN

M. Kimura[3], S. Aghion[1,2], C. Amsler[3], A. Ariga[3], T. Ariga[3],
A. Belov[4], G. Bonomi[5,6], P. Bräunig[7], J. Bremer[8], R. S. Brusa[9,10],
L. Cabaret[11], M. Caccia[12,2], R. Caravita[13,14], F. Castelli[15,2],
G. Cerchiari[16], K. Chlouba[17], S. Cialdi[15,2], D. Comparat[11],
G. Consolati[1,2], A. Demetrio[7], H. Derking[8], L. Di Noto[13,14],
M. Doser[8], A. Dudarev[8], A. Ereditato[3], R. Ferragut[1,2], A. Fontana[6],
S. Gerber[8], M. Giammarchi[2], A. Gligorova[18], S. Gninenko[4],
S. Haider[8], H. Holmestad[19], T. Huse[19], E. J. Jordan[16], J. Kawada[3],
A. Kellerbauer[16], D. Krasnicky[13,14], V. Lagomarsino[13,14], S. Lehner[20],
C. Malbrunot[8,20], S. Mariazzi[20], V. Matveev[4], Z. Mazzotta[15,2],
G. Nebbia[21], P. Nedelec[22], M. Oberthaler[7], N. Pacifico[18],
D. Pagano[5,6], L. Penasa[9,10], V. Petracek[17], C. Pistillo[3], F. Prelz[2],
M. Prevedelli[23], L. Ravelli[9,10], C. Riccardi[24,6], O. M. Røhne[19],
S. Rosenberger[8], A. Rotondi[24,6], M. Sacerdoti[2], H. Sandaker[19],
R. Santoro[12,2], P. Scampoli[3,25], F. Sorrentino[14], M. Spacek[17],
I. M. Strojek[17], J. Storey[3], M. Subieta[5,6], G. Testera[14],
E. Widmann[20], P. Yzombard[11], S. Zavatarelli[14], J. Zmeskal[20] (AEgIS
collaboration)

E-mail: `mitsuhiro.kimura@lhep.unibe.ch`
[1] Politecnico of Milano, Piazza Leonardo da Vinci 32, 20133 Milano, Italy
[2] INFN Milano, Via Celoria 16, 20133 Milano, Italy
[3] Laboratory for High Energy Physics, Albert Einstein Center for Fundamental Physics,
University of Bern, 3012 Bern, Switzerland
[4] Institute for Nuclear Research of the Russian Academy of Science, Moscow 117312, Russia
[5] Department of Mechanical and Industrial Engineering, University of Brescia, Via Branze 38,
25123 Brescia, Italy
[6] INFN Pavia, Via Bassi 6, 27100 Pavia, Italy
[7] Kirchhoff-Institute for Physics, Heidelberg University, Im Neuenheimer Feld 227, 69120
Heidelberg, Germany
[8] Physics Department, CERN, 1211 Geneva 23, Switzerland
[9] Department of Physics, University of Trento, Via Sommarive 14, 38123 Povo, Trento, Italy
[10] TIFPA/INFN Trento, Via Sommarive 14, 38123 Povo, Trento, Italy
[11] Laboratory Aimé Cotton, CNRS, University of Paris-Sud, ENS Cachan, Bât. 505, 91405
Orsay, France
[12] Department of Science, University of Insubria, Via Valleggio 11, 22100 Como, Italy
[13] Department of Physics, University of Genova, Via Dodecaneso 33, 16146 Genova, Italy
[14] INFN Genova, Via Dodecaneso 33, 16146 Genova, Italy
[15] Department of Physics, University of Milano, Via Celoria 16, 20133 Milano, Italy
[16] Max Planck Institute for Nuclear Physics, Saupfercheckweg 1, 69117 Heidelberg, Germany
[17] Czech Technical University, Prague, Brehová 7, 11519 Prague 1, Czech Republic
[18] Institute of Physics and Technology, University of Bergen, Allégaten 55, 5007 Bergen,
Norway

[19] Department of Physics, University of Oslo, Sem Sælandsvei 24, 0371 Oslo, Norway

[20] Stefan Meyer Institute for Subatomic Physics, Austrian Academy of Sciences, Boltzmanngasse 3, 1090 Vienna, Austria

[21] INFN Padova, Via Marzolo 8, 35131 Padova, Italy

[22] Institute of Nuclear Physics, CNRS/IN2p3, University of Lyon 1, 69622 Villeurbanne, France

[23] University of Bologna, Viale Berti Pichat 6/2, 40126 Bologna, Italy

[24] Department of Physics, University of Pavia, Via Bassi 6, 27100 Pavia, Italy

[25] Department of Physics, University of Napoli Federico II, Complesso Universitario di Monte S. Angelo, 80126, Napoli, Italy

Abstract. The goal of the AEgIS experiment is to measure the gravitational acceleration of antihydrogen – the simplest atom consisting entirely of antimatter – with the ultimate precision of 1%. We plan to verify the Weak Equivalence Principle (WEP), one of the fundamental laws of nature, with an antimatter beam. The experiment consists of a positron accumulator, an antiproton trap and a Stark accelerator in a solenoidal magnetic field to form and accelerate a pulsed beam of antihydrogen atoms towards a free-fall detector. The antihydrogen beam passes through a moiré deflectometer to measure the vertical displacement due to the gravitational force. A position and time sensitive hybrid detector registers the annihilation points of the antihydrogen atoms and their time-of-flight. The detection principle has been successfully tested with antiprotons and a miniature moiré deflectometer coupled to a nuclear emulsion detector.

1. Introduction

Three centuries after Newton first described the properties of the gravitation force our knowledge of gravity is still limited to Einstein's theory of General Relativity, as a consistent quantum theory of gravity has not been developed yet. General Relativity is based on the Weak Equivalence Principle (WEP) that is, the universality of gravitational free-fall. This principle has been tested with precisions down to 10^{-13} by Eötvös-type experiments using probes made of matter. The WEP also requires antimatter to fall with the same acceleration as matter, but no precise direct measurements have been made so far [1].

On the other hand, extensions of the standard model which attempt to quantize gravity suggest a difference between the gravitational acceleration g of matter and $\bar{g}$, that of antimatter [2]. A violation of the WEP by antimatter would lead to new physics beyond General Relativity.

The goal of the AEgIS experiment at CERN (Antimatter Experiment: Gravity, Interferometry, Spectroscopy) is to test the Weak Equivalence Principle with antihydrogen in the gravitational field of the Earth [3]. The experiment plans a direct measurement of the gravitational acceleration of antihydrogen ($\overline{\text{H}}$) atoms with an ultimate accuray of 1%. Using electrically neutral systems such as antihydrogen (made of an antiproton $\bar{\text{p}}$ and a positron e^+) minimizes the disturbance from electromagnetic stray fields. The gravity measurement will be carried out by first forming an antihydrogen beam and then observing its vertical displacement with a moiré deflectometer.

The AEgIS collaboration is designing and building the equipment and it is currently taking data at CERN's Antiproton Decelerator (AD). Details on the apparatus are reported in this paper, together with a proof of principle established with antiprotons.

2. Overview of the AEgIS experiment

The basic principle of the AEgIS experiment is shown in figure 1. The AD produces 5.3 MeV antiprotons which are degraded in an absorber to maximize the capture efficiency in the antiproton capture trap. Positrons derived from a ^{22}Na source are first accumulated and then accelerated towards nanoporous material which produce positronium (Ps).
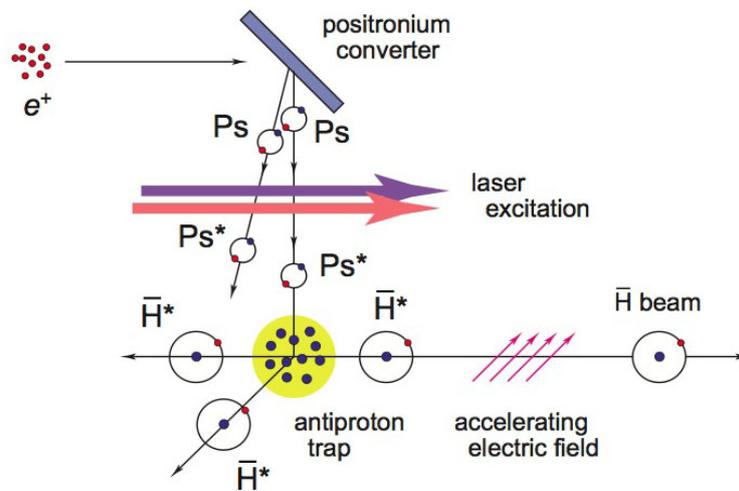
Figure 1. Principle of antihydrogen production in AEgIS.

Antihydrogen production.   Rydberg antihydrogen atoms $\overline{\mathrm{H}}^*$ are produced from cold antiprotons ($\overline{\mathrm{p}}$) and Rydberg (ortho)positronium Ps^* via the charge exchange reaction $\mathrm{Ps}^* + \overline{\mathrm{p}} \to \overline{\mathrm{H}}^* + \mathrm{e}^-$ [4, 5]. This process has various advantages:

- The production cross section scales as $\sigma \propto n_{\mathrm{Ps}}^4$ where n_{Ps} is the principal quantum number of orthopositronium. The cross section is around 10^{-9} cm^2 for $n_{\mathrm{Ps}} = 20$.
- The reaction can produce ultracold antihydrogen atoms if the antiprotons are cold enough. The antihydrogen temperature is 120 mK for $T_{\overline{\mathrm{p}}} = 100$ mK and $n_{\mathrm{Ps}} = 30$.
- The antihydrogen atoms are pulsed. The temperature of the antihydrogen atoms must be low enough ($\sim$100 mK) to reduce the beam spread (Maxwell-Boltzmann distribution with the average speed of 50 m/s).

Antihydrogen beam formation.   The antihydrogen atoms in excited Rydberg states have large electric dipole moments and can be accelerated by electric field gradients to several 100 m/s towards the moiré deflectometer. This technique has already been demonstrated by accelerating Rydberg hydrogen atoms with $n = 22, 23, 24$ to velocities up to 2×10^8 m/s^2 [6].

Gravity measurement.   The gravity module, a classical moiré deflectometer [7] coupled to an $\overline{\mathrm{H}}$ detector, will measure the gravitational acceleration $\overline{g}$ of the antihydrogen beam. The deflectometer consists of two silicon gratings of 40 µm pitch with 12 µm slit widths. The two gratings are 40 cm apart. Figure 2 shows that the two gratings produce a pattern on the $\overline{\mathrm{H}}$ detector with the same period as the grating pitch. The intensity pattern can be measured precisely with emulsion detectors (see below).

   The trajectory of the $\overline{\mathrm{H}}$ atoms is affected by gravity, which leads to a shift of the periodic pattern, depending on the strength of the gravitational force and the velocity of the beam between the two gratings. The shift is determined by including a measurement of the time-of-flight between the production point and the detector. The gravitational acceleration $\overline{g}$ is given
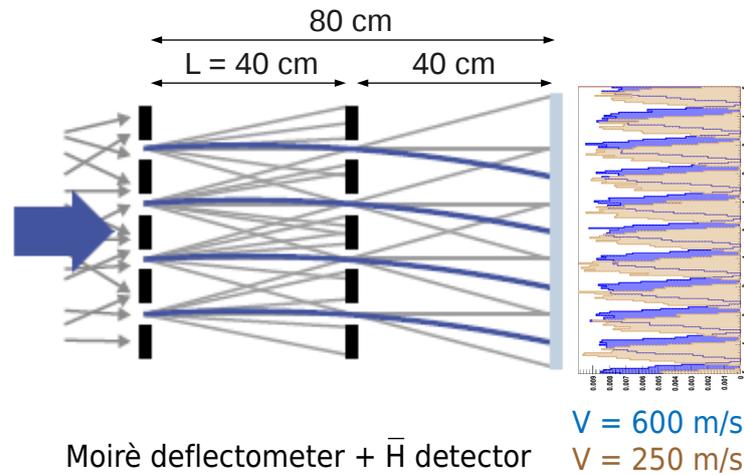
Figure 2. Moiré deflectometer and $\overline{\mathrm{H}}$ detector. Antihydrogen atoms annihilating on the detector surface generate a periodic pattern. A shift of the pattern is caused by the vertical gravitational force.

by

$$\delta x = -\overline{g}\frac{L^2}{v^2}$$

where δx is the vertical shift of the periodic pattern, L the distance between the gratings, and v the velocity of the $\overline{\mathrm{H}}$ atom.

The $\overline{\mathrm{H}}$ detector combines a position sensitive detector with a time-of-flight detector. To achieve our ultimate goal of a 1% relative error on $\overline{g}$ within a reasonable time the detector pitch should be around 40 μm. The time-of-flight needs to be measured with resolutions at the sub-microsecond level.

3. The AEgIS apparatus

The AEgIS apparatus is located in the CERN-AD hall. Figure 3 shows a sketch of the equipment consisting of the positron accumulator, the antiproton trapping system, the cryogenic system in ultrahigh vacuum (UHV), two superconductive solenoids supplying fields of 5 T and 1 T, and the gravity module. Most of the apparatus is already installed while the gravity module is under design. Data taking and commissioning with antiprotons started in 2012.

Antiproton. The charge exchange reaction to form antihydrogen requires cold antiprotons and Rydberg positronium atoms. The AD provides 3×10^7 antiprotons every 100 s. A thin aluminium degrader foil reduces the kinetic energy of the antiprotons from 5.3 MeV to about 100 keV. Typically 10^5 antiprotons are caught by a Penning-Malmberg trap [8], among which 90% should be cooled down to 0.1 K in the 5 T magnet. The temperature currently reached in the trap is 7 K. We intend to reach 0.1 K by combining electron cooling (0.7 K can be achieved) with other methods such as a resistive cooling and laser cooling [9].

Positron. The Surko type [10] positron accumulator system consists of a 50 mCi ^{22}Na source, a solid neon moderator, a CO_2 buffer gas trap, and an accumulator. The moderator produces
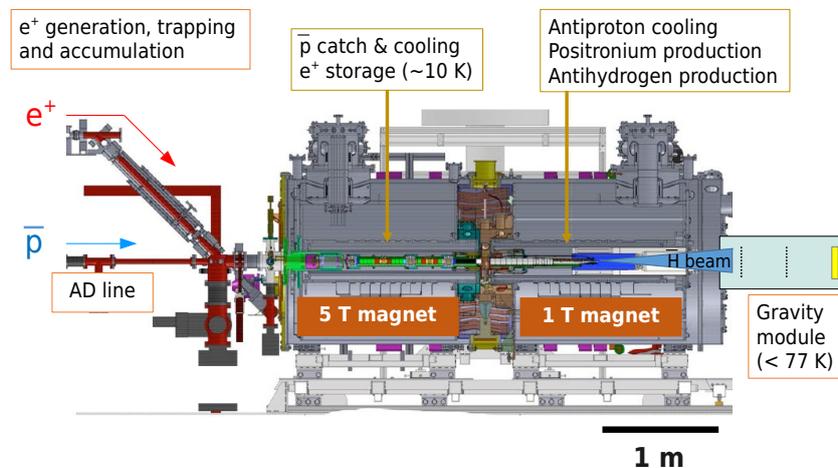
Figure 3. Sketch of the AEgIS apparatus. The two lines send positrons and antiprotons towards the main magnets of 5 T and 1 T. The 5 T magnet is equipped with an unique trap to hold the antiprotons and the positrons. In the 1 T region antihydrogen atoms can be formed and accelerated towards the gravity module.

a slow positron beam of a few eV by reducing the energy of the positrons from the radioactive source. The accumulator can stack 4×10^7 positrons in a few minutes. The beam transport system is being optimized to increase the positron intensity.

Positronium. Positronium is produced by irradiating with positrons a silicon substrate perforated with nanochannels of 8 – 14 nm diameters [11]. Aerogel is also studied as an alternative to silicon. The cross section of the reaction $Ps^* + \overline{p} \to \overline{H}^* + e^-$ is high whenever the relative velocity between antiproton and positron are matched. The formation efficiency is typically 9% for 7 keV positrons and a silicon target at 150 K.

Rydberg positronium. Positronium is excited from $n_{Ps} = 1$ to $n_{Ps} = 25$ by a laser system providing of two laser pulses [12, 13]. A 205 nm UV laser induces the transition $n_{Ps} = 1$ to $n_{Ps} = 3$ and a 1650 – 1700 nm IR laser subsequently excites the $n_{Ps} = 25$ level.

Antihydrogen detector. Ultra-cold antihydrogen atoms are produced by the charge exchange process between Rydberg positronium and cold antiprotons in the 1 T magnet. The Fast Annihilation Cryogenic Tracking detector (FACT) monitors the formation of antihydrogen atoms in the UHV at 4 K and in the 1 T magnetic field [14]. Figure 4 shows the detector designed to sample the antihydrogen cloud and to measure some of its properties. The FACT reconstructs the $\overline{H}$ annihilation point along the axis from the tracks of the charged pions emitted when the $\overline{H}$ atoms hit the inner cryostat walls (or annihilate in the rest gas). The detector consists of 800 scintillating (1 mm diameter) fibers coupled to clear fibers to transport the scintillation light to Hamamatsu MPPC silicon photomultipliers. The vertex reconstruction accuracy along the beam axis is 2.1 mm, based on GEANT4 simulations [14].

The detector was installed in the 1 T magnet in August 2014. A UV LED was incorporated to calibrate and check the detector performance. The detector response to the UV light at room temperature and at 37 K shows that the detector is correctly performing at cryogenic

temperatures. Antiproton data were collected in December 2014, the analysis of which is underway.
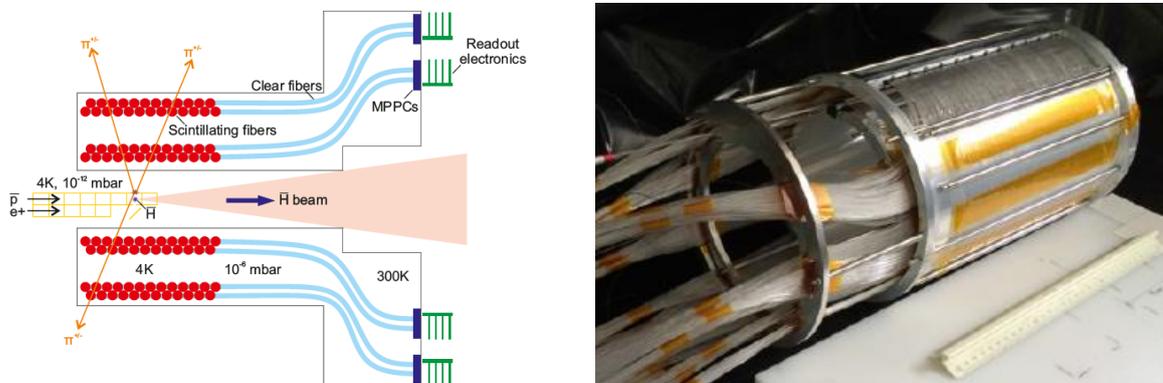

Figure 4. Left: diagram of the FACT detector. Right: photograph of the FACT scintillation fiber detector which measures the coordinate of the $\overline{\text{H}}$ annihilation vertex along the axis.

Gravity module. The design of the gravity module is in progress. The sensitivity on $\bar{g}$ depends on the position resolution and on the number of detected antihydrogen atoms. The expected precision $\Delta\bar{g}/\bar{g}$ is shown in figure 5 as a function of the number of detected annihilations [15]. Compared to the original AEgIS proposal [3] the improvement on the position resolution, essentially due to the use of emulsions, reduces considerably the time required to achieve the 1% accuracy. Indeed, emulsion films provide outstanding sub-micron resolutions [16, 17]. An emulsion film is made of a 200 μm thick plastic base with 50 μm thick emulsion layers on both surfaces. The initial diameter of silver bromide (AgBr) crystals embedded in the emulsion layer is 200 nm. The photographic development increases the size of the silver grains to 600 nm, thus allowing the track to be observed with an optical microscope.

Figure 6 (left) shows the photograph of a stopping (∼100 keV) antiproton annihilating on the emulsion surface. The emulsion film has been scanned and analyzed by the automatic scanning microscope [18, 19] at the University of Bern. The impact parameter distribution of reconstructed vertices on the bare emulsion and on an emulsion film covered by a 20 μm thick stainless steel foil are shown in figure 6 (right). The root mean square (rms) resolution is 1 – 2 μm.

However, further information is needed from a time-of-flight device. A possible layout of the hybrid detector is shown in figure 7. It would consist of three layers of silicon strips [20, 21], followed by emulsion films and a scintillating fiber tracker. The silicon strip detector would be an active 50 μm thick annihilation foil, required to separate the UHV from the ordinary vacuum region containing the emulsion detector, as well as providing timing and rough position information. The time resolution is of the order of a few ns and the rms position resolution of strips around 10 μm. The emulsion films improve the resolution on the annihilation vertex by an order of magnitude. The scintillating fibers consisting of two $x - y$ provide additional redundant information on the approximate vertex position and on the time-of-flight.

A moiré pattern can be imprinted on the emulsion by shining light through a transparent window in the silicon detector, thus aligning the emulsions to the deflectometer. The detectors themselves are aligned with the charged pions emitted from antiproton annihilation (average momentum of 0.3 GeV/c).
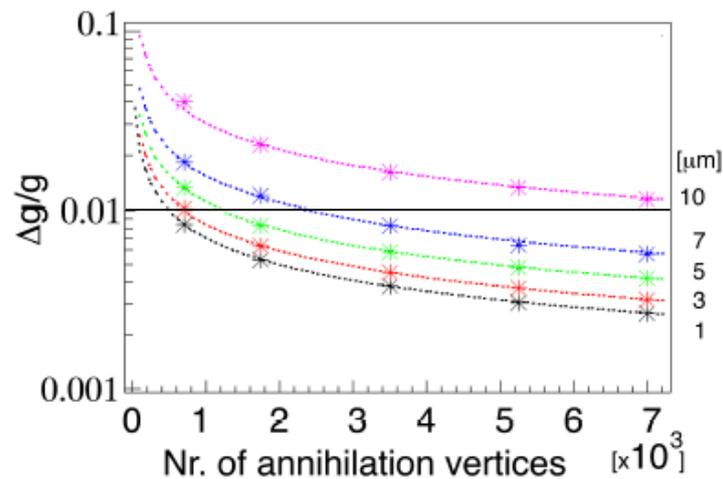
Figure 5. Simulated relative sensitivity on $\overline{g}$ as function of detected antihydrogen vertices. The numbers on the right indicate the corresponding resolution of the position sensitive detector. The horizontal black line shows the ultimate goal of 1%.
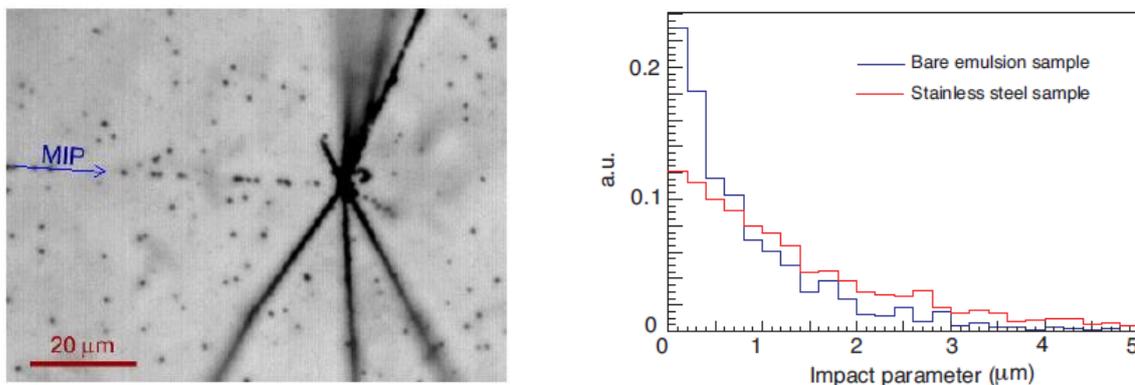

Figure 6. Microscopic view of an antiproton annihilation vertex (star) in the emulsion (left) and impact parameter distribution of the reconstructed vertices (right) on the bare emulsion surface and in the 20 μm thick stainless steel foil.

4. Proof of principle

We have exposed a miniature copy of the moiré deflectometer ("mini-moiré") coupled to an emulsion detector by using antiprotons from the AD. The deflectometer contained two different regions, a single grating zone in direct contact with the emulsion, and a moiré zone consisting of a pair of gratings separated by 25 mm. The test was performed in December 2012 [22]. The kinetic energy of the degraded antiproton beam was around 100 keV, based on GEANT4 simulations. The reference pattern for the alignment was made by exposing the gratings and the emulsion films to visible light.

A total of 241 annihilation stars were reconstructed in the emulsions, the position of which
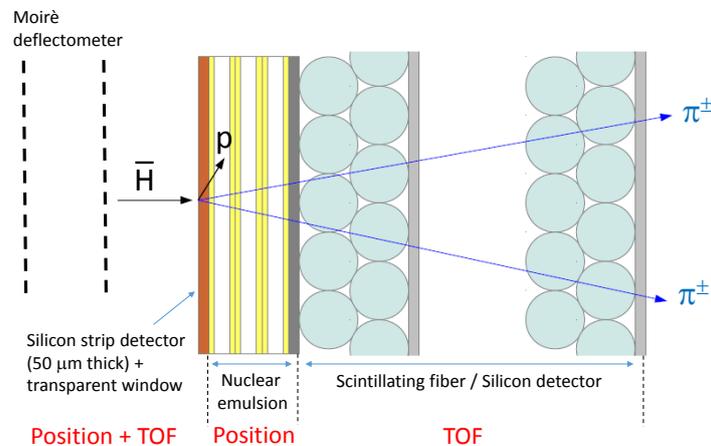
Figure 7. A design of the hybrid $\overline{\overline{\text{H}}}$ detector.

was determined with a 2 μm rms uncertainty. The distribution of the annihilation vertices was then compared to the reference light pattern. Both patterns are shown in figure 8(a). Figure 8(b) (top left) shows the distribution in the moiré zone. Figure 8(b) (top right) shows the contact single grating region, which is used to align the antiproton and light measurements. Figure 8(c) shows the number of detected antiprotons in the moiré zone as a function of vertical coordinate y (in grating units d). The period of the moiré pattern from antiprotons was found to be the same as the reference light pattern, but shifted by $9.8 \pm 0.9(\text{stat}) \pm 6.4(\text{syst})$ μm. The shift of the moiré pattern is consistent with a mean force of $530 \pm 50(\text{stat}) \pm 350(\text{syst})$ aN acting on the antiprotons, corresponding to a Lorentz force generated by a 7.4 G magnetic field. The force is due to the fringing field of the 1 T magnet measured to be about 10 G at the mini-moiré location.

We have thus demonstrated that a deflectometer coupled to a high resolution position detector is able to measure a micrometric shift. The gravitational force acting on antihydrogen is 10 orders of magnitude smaller than the magnetic force experienced here. However, the setup foreseen in the AEgIS proposal assumes a antihydrogen beam with $\overline{\text{H}}$ atoms moving at several hundred m/s, passing through a 80 cm long moiré deflectometer. The expected shift due to gravity is then comparable to the one observed in this test experiment.

5. Conclusions and outlook

The goal of the AEgIS experiment is to measure the gravitational acceleration of antihydrogen with 1% accuracy and test the Weak Equivalence Principle which lies at the base of General Relativity. Most of the equipment has been installed with the exception of the gravity module which is still the subject of research and development. We have performed a test experiment with a miniature copy of the gravity module. The results have shown that a micrometric shift is observable, and thus establish the feasibility of the proposed detection method. Obviously, the short term plan is to produce antihydrogen atoms. This requires improvements in antiproton cooling system, in the positron system and the optimization of positronium production. The goal is to produce an antihydrogen beam in 2015–2016 and to perform a first rough measurement of the gravitational acceleration shortly thereafter.
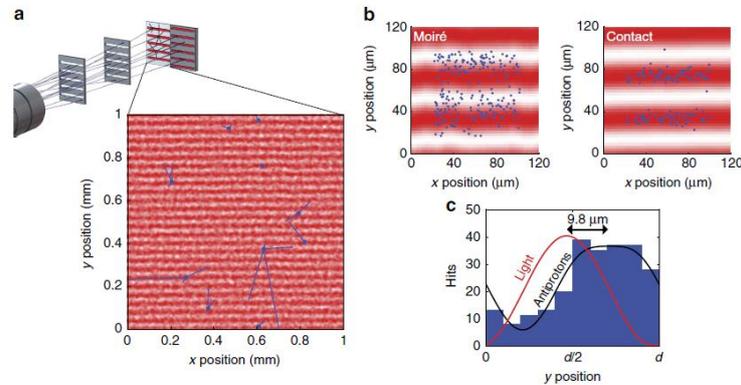
Figure 8. (a) Sketch of the mini-moiré and the emulsion detector. The antiprotons pass through the mini-moiré deflectometer and annihilate on the emulsion detector. (b) Comparison of the light patterns: the reference pattern and the annihilation pattern are plotted as blue dots and red fringes, respectively. The antiproton vertices in the moiré zone are shown in the left square, the ones in the contact region in right square. (c) Observed shift of the antiproton pattern in the moiré region due to the Lorentz force (reprinted figures from ref. [22]. Copyright (2014) by Macmillan Publishers Limited. DOI: 10.1038/ncomms5538).

References

[1] C. Amole *et al.* (ALPHA Collaboration), Nature Communications 4 (2013) 1785
[2] K. Jagannathan and L. P. S. Singh, Phys. Rev. D33 (1986) 2475
[3] G. Drobychev *et al.*, 2007 CERN-SPSC-2007017,
    http://cdsweb.cern.ch/record/1037532
[4] M. Charlton, Phys. Lett. A 143 (1990) 143
[5] C. H. Storry *et al.*, Phys. Rev. Lett. 93 (2004) 263401
[6] E. Vliegen, F. Merkt, J. Phys. B 39 (2006) L241
[7] M. K. Oberthaler *et al.*, Phys. Rev. A 54 (1996) 3165
[8] D. Krasnický *et al.* (AEgIS Collaboration), AIP Conf. Proc. 1521, 144 (2013)
[9] A. Kellerbauer and J. Walz, New J. Phys. 8 (2006) 45
[10] C. M. Surko *et al.*, Phys. Rev. Lett. 62, 901 (1989)
[11] S. Mariazzi *et al.*, Phys. Rev. B. 81, 235418 (2010)
[12] F. Castelli *et al.*, Phys. Rev. A 78 (2008) 052512
[13] S. Cialdi *et al.*, Nuclear Instruments and Methods in Physics Research B 269 (2011) 1527
[14] J. Storey *et al.* (AEgIS Collaboration), Nuclear Instruments and Methods in Physics Research A 732 (2013) 437
[15] S. Aghion *et al.* (AEgIS Collaboration), JINST 8 P08013 (2013)
[16] C. Amsler *et al.*, J. of Instrumentation 8 (2013) P02015
[17] M. Kimura *et al.*, Nuclear Instruments and Methods in Physics Research A 732 (2013) 325
[18] S. Aoki *et al.*, Nuclear Instruments and Methods B 51 (1990) 466.
[19] L. Arrabito *et al.*, Nuclear Instruments and Methods A 568 (2006) 578
[20] S. Aghion *et al.* (AEgIS Collaboration), J. of Instrumentation 9 (2014) P06020
[21] N. Pacifico *et al.*, Nuclear Instruments and Methods in Physics Research A 765 (2014) 161
[22] S. Aghion *et al.* (AEgIS Collaboration), Nature Communications 5 (2014) 4538